MULTIEXCITATION HYPERSPECTRAL IMAGING TOWARD IMPROVED LICHEN IDENTIFICATION

Narek Chilingaryan[1], *Arsen Gasparyan*[2,3], *Narine Sarvazyan*[1,2,4]

[1]Orbeli Institute of Physiology NAS RA, Yerevan, Armenia
[2]American University of Armenia, Yerevan, Armenia
[3]Institute of Botany after A. Takhtajyan NAS RA, Yerevan, Armenia
[4]George Washington University, Washington, DC, United States

ABSTRACT

Hyperspectral imaging (HSI) has significantly advanced the identification and characterization of biological specimens by utilizing high-resolution data across multiple spectral bands. In the study of lichens, which are symbiotic entities formed by fungi and photosynthetic partners, our novel approach leverages the potential of HSI through a technique referred to as multi-excitation HSI (ME-HSI). This method differentiates itself by employing multiple ultraviolet wavelengths for illumination, capturing data in the visible range, and subsequently integrating these hyperspectral cubes. Our research demonstrates that this innovative technique provides superior effectiveness in identifying lichen species. By detailing unique spectral signatures, ME-HSI facilitates species differentiation, enhancing the accuracy of ecological monitoring and conservation efforts through non-invasive methods.

Index Terms— Hyperspectral Imaging, Autofluorescence, Lichenology, Taxonomy, Environment

1. INTRODUCTION

Lichens play a critical role as bioindicators due to their sensitivity to environmental changes and pollutants. They contribute to ecosystem health by participating in nutrient cycling and soil formation [1]. In Armenia, a region with diverse climatic zones and rich biodiversity, the accurate identification and monitoring of lichens are particularly crucial [2]. Lichen diversity in Armenia not only reflects the region's unique ecological conditions but also provides insights into environmental changes and the impacts of anthropogenic activities. However, identifying different lichen species is notoriously difficult given their visual similarities and complex structures [3]. Our research seeks to address these needs by advancing identification methods through multi-excitation hyperspectral imaging (ME-HSI). In the past, reflectance-based hyperspectral imaging has shown to be effective for daylight aerial monitoring of lichen growth and distribution [4]. However, this approach works only for lichen species that exhibit significant differences in their reflectance spectra, i.e., their color. Yet many species of lichens are indistinguishable by color in which case additional physical factors or properties needs to be explored.

The ability to rapidly and straightforwardly differentiate species using HSI is especially useful for researchers focused on ecological monitoring, biodiversity, lichen conservation efforts and sustainable ecosystem management. Here we focus on the use of ME-HSI, which employs multiple ultraviolet and visible wavelengths to illuminate the samples while capturing images in the visible range. Using this approach, we attempted to differentiate three species of lichens that are visually indistinguishable color-wise. The data have confirmed the enhanced capacity of ME-HSI to reveal subtle spectral differences. Our findings support the use of ME-HSI for ecological and preservation purposes, going beyond current remote sensing paradigms.

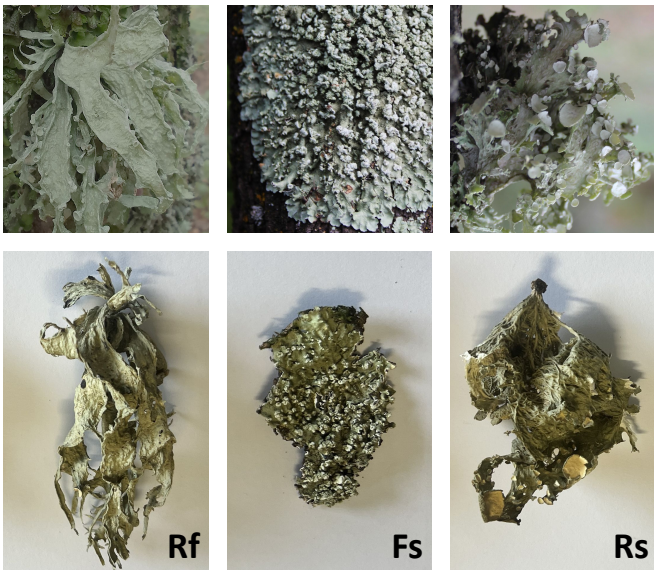

Fig. 1: Images of three lichen species in the wild and as a dried specimen. Label Rf stands for Ramalina fraxinea , Fs for Flavopunctelia soredica, and Rs for Ramalina sinensis. Upper row photographs are courtesy of Naira Sargsyan.

2. MATERIALS AND METHODS

2.1. Collection and identification of lichens

The selected lichen samples of Ramalina sinensis Jatta, Ramalina fraxinea (L.) Ach., and Flavopunctelia soredica (Nyl.) Hale were the subject of this study (Fig. 1). The material was collected from the territory of the Republic of Armenia. Species identification was carried out using standard methods and based on commonly used identification guides and keys [5, 2]. The nomenclature follows Index Fungorum (www.indexfungorum.org).

2.2. Imaging setup

Dried lichen samples were cut into approximately 5 mm × 5 mm squares and positioned on a black background to ensure optimal contrast and to reduce influence from ambient reflections, providing a consistent baseline for spectral analysis. For illumination, we used a rotatable wheel (Mightex Systems, WLS-23-A) containing eight UV-VIS LEDs with wavelengths ranging from 310 to 430 nm and the broadband 5500K cool white LED Fig. 2. Hyperspectral images were acquired within 420-720 range with either 2 or 10 nm spectral resolution using the Nuance FX Imaging System (CRi, Woburn, MA, USA).

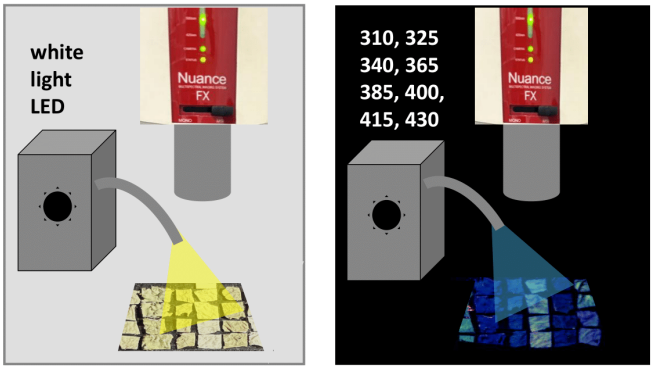

Fig. 2: Cartoon depiction of the reflectance (left) and autofluorescence HSI (right) setups used in this study.

2.3. Linear Unmixing

Image processing was performed using the proprietary Nuance 3.0.2 software. The first set of analysis involved sequential analysis of individual HSI datacubes each obtained under different illumination conditions. To create spectral libraries small square regions of interest (2 mm × 2 mm) were placed on each type of lichen and the spectral profiles from each species were then used to apply to the rest of the HSI dataset. Linear unmixing based on the spectral proximity of unknown spectra to the extracted spectral profiles was then performed using Nuance 3.0.2 software (PerkinElmer).

2.4. k-NN classification

Data was processed using custom-written Python scripts and the "scikit-learn" machine learning library (version 1.6.1) [6]

2.4.1. Data preprocessing and HSI configurations

Data was initially corrected at datacube level by acquisition exposure time to bring each datacube to a similar level of signal. Preprocessing then branched into (a) pixel-level SNV (standard normal variate) normalization within each datacube resulting in the single-excitation configurations of data, denoted by excitation conditions, (b) concatenation of these normalized spectra to obtain one of the multi-excitation configurations, denoted *NC* (normalization-then-concatenation), and (c) concatenation of non pixelwise-normalized spectra to obtain the other multi-excitation configuration, denoted as *CN* (concatenation-then-normalization). Two versions were implemented: one by concatenating eight datacubes (with 310, 325, 340, 365, 385, 400, 415, and 430 nm excitation wavelengths), resulting in the *NC_8* and *CN_8* configurations, and another by concatenating three datacubes (340, 365, and 385 nm), yielding the *NC_3* and *CN_3* configurations. Finally, before the application of the k-nearest neighbors algorithm (k-NN), feature scaling was performed per configuration, where features are emission wavelengths, and samples are pixels.

2.4.2. Cross-validation and image-wise classification

For cross-validation (CV) and model selection, regions of interest (ROIs) were selected to comprise the train set of data (Fig. 5b, top-left image). For quantification purposes, only the lichen regions were included in cross-validation because the background material and the reflectance standard are quite different spectra-wise and by their inclusion one can overrepresent the classification metrics. Grid search was performed for each HSI configuration using 5-fold cross-validation, testing k-neighbors from 5 to 500, with the evaluation metric being the balanced accuracy (BA, the average recall rate across classes). For image-wise classification, k-NN with 5 neighbors was chosen, based on the highest average BA across different HSI configurations. CV scores between HSI configurations were compared using two-sided independent t-test.

3. RESULTS AND DISCUSSION

3.1. Reflectance-based HSI

The initial series of experiments aimed to assess the effectiveness of reflectance-based HSI in distinguishing individual lichen species. Samples were illuminated using the cool white LED source while capturing images within the 420 to 720 nm spectral range with resolutions of either 10 or 2 nm. Although some insights were gleaned from the analysis of these spectral

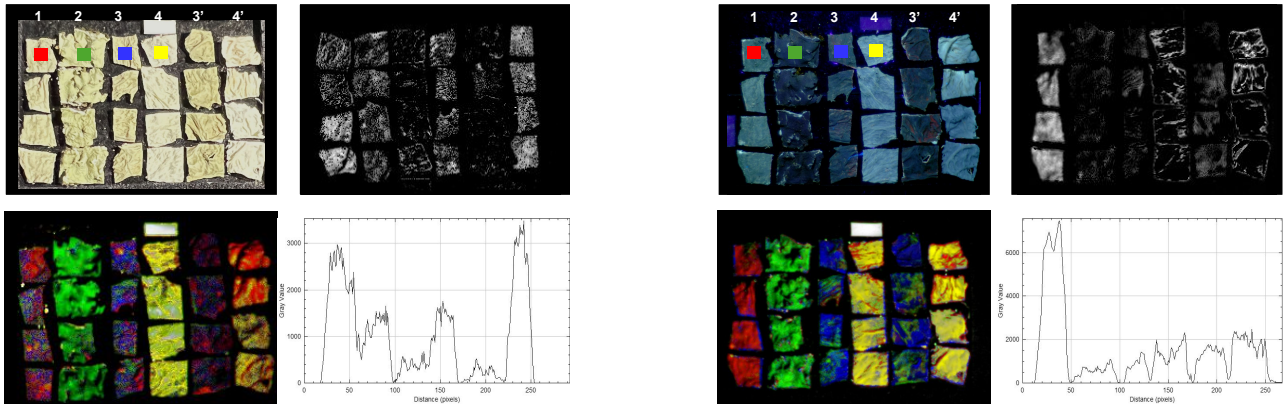

(a) Visual outcomes of reflectance HSI.

(b) Visual outcomes of autofluorescence HSI at 385 nm.

Fig. 3: Comparative visual outcomes of linear unmixing based on reflectance (a) vs autofluorescence HSI (b). Panels on top left show the appearance of lichen samples under daylight and UV light respectively. The numbers on the top indicate lichen species with 1 being Rf, 2–Fs, 3–Rs, 4–back side of Rs, 3'–another sample of Rs, 4'–another sample of Rs backside. The bottom left panels show the outcome of linear unmixing by Nuance 3.0.2 algorithm using spectra extracted from color boxes shown in the panel above. The gray images on the right illustrates the component images corresponding to the sample 1 spectrum. Finally, graphs on the bottom right depict the intensity distribution of sample 1 component across the entire field.

cubes, the spectral unmixing quality was found to be suboptimal (Fig. 3a).

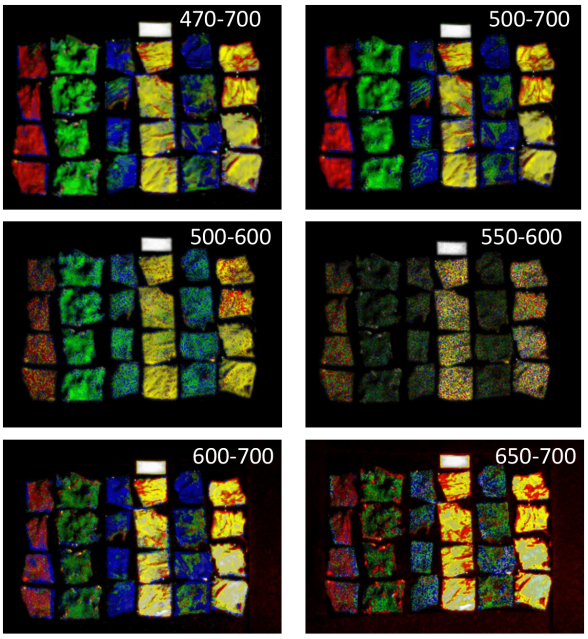

Fig. 4: Decline of identification accuracy upon shortening of the emission range. The quality of unmixing can be judged qualitatively by 1) pseudocolor intensity within each column that has identical species; 2) correct separation of samples in columns I, II, III and IV, 3) degree of correct identification of column V based on spectrum from column III, and column VI based on spectrum from column IV.

3.2. Autofluorescence-based HSI: single excitation approach

Biological fluorophores exhibit excitation across a broad spectrum, with the ultraviolet/blue region being particularly prevalent [7]. To identify the optimal excitation wavelength, we tested eight LEDs ranging from 300 to 430 nm (Fig. 3b) while capturing images within a range starting from 50 nm beyond the illuminating light wavelength. This adjustment was made to prevent signal oversaturation caused by the direct contribution of the illuminating light source from its spectral tail. Enhanced target identification was observed with increasing excitation wavelength, culminating in optimal results at 400-430 nm. The width of the emission spectra also influenced the unmixing quality, as qualitatively depicted in Fig. 4.

Next, we confirmed the above findings quantitively using k-NN approach detailed below. We also statistically tested the hypothesis that combining HSI datacubes from multiple excitation sources can increase classification effectiveness. Multi-excitation HSI (ME-HSI) effectively expands the traditional 3D HSI cube into the fourth dimension. By concatenating these cubes into a consolidated new 3D cube or analyzing the data as excitation-emission matrices, a more effective spectrum unmixing process can be achieved.

3.3. k-NN Classification

Cross-validation within the training set (Fig. 5b, top left image) showed increased performance towards higher excitation wavelengths when excitation by individual wavelength was used (Fig. 5). In this configuration, the highest perfor-

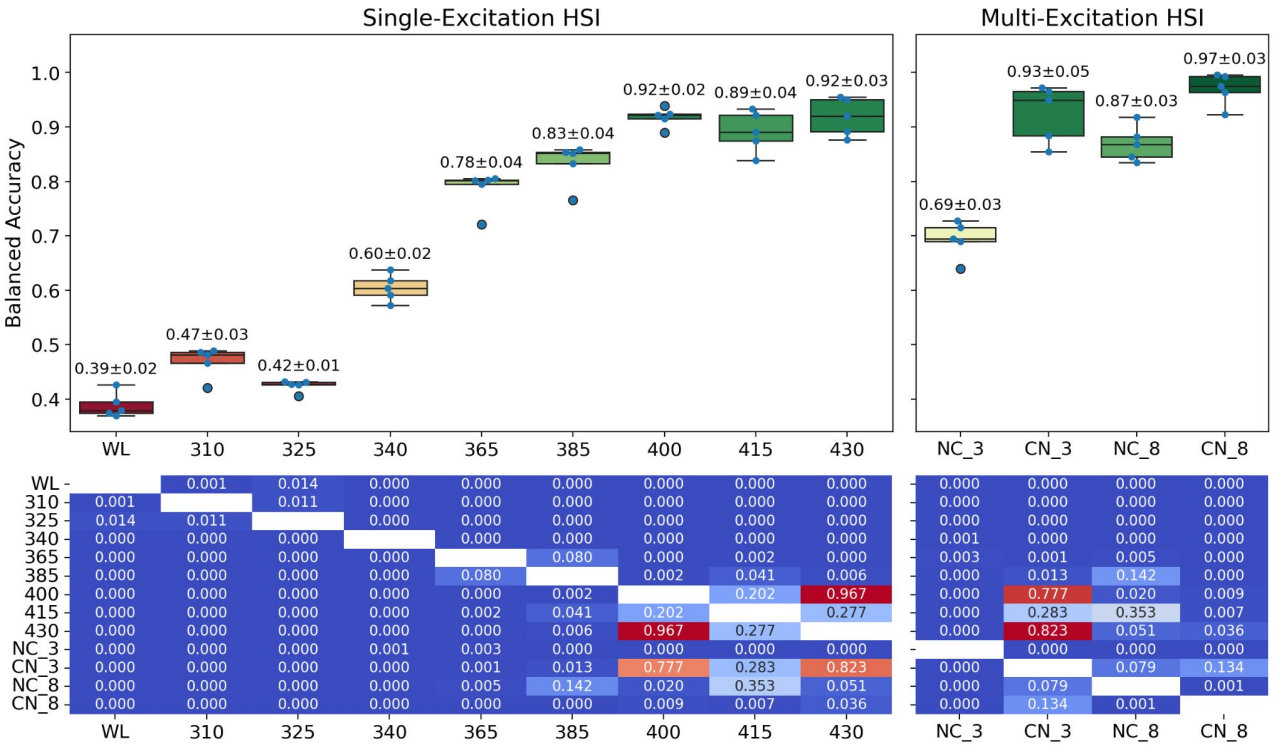

(a) Boxplots visualize the cross-validation scores for 5-fold splits of the train data, represented by the mean and the standard deviation. Heatmaps provide the p-values from pairwise comparisons between all groups.

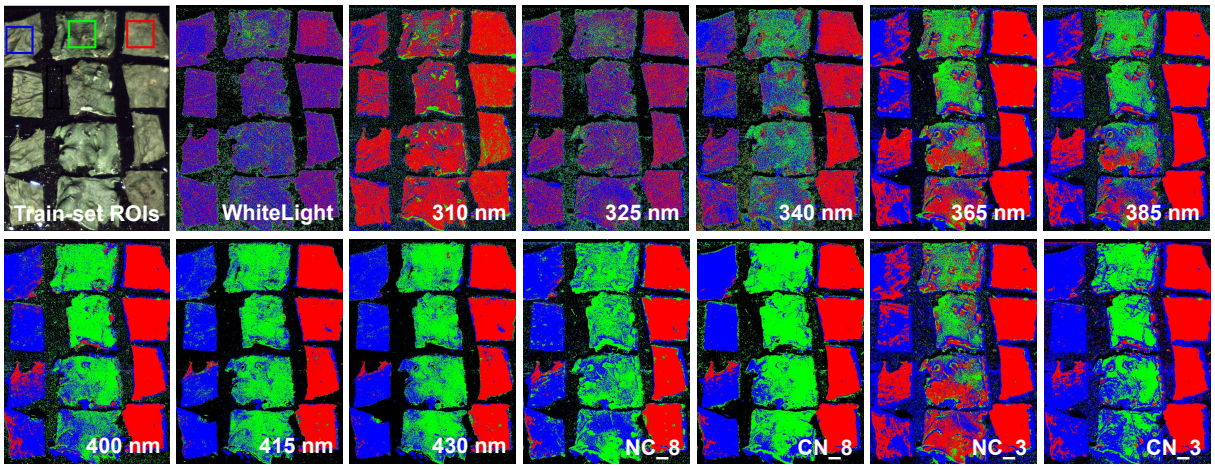

(b) Visual representation of image-wide pixel classification. The ROIs in the top left image were used for both—cross-validation (Fig. 5a), and training the k-NN model for image-wide classification.

Fig. 5: k-NN classification performed on single- and multi-excitation HSI configurations with 5 k-neighbors. *NC* and *CN* stand for normalization-then-concatenation and concatenation-then-normalization processing approaches respectively. Following the underscore is the number of single-excitation datacubes concatenated to form the ME-HSI configuration: 8 indicates all single-excitation cubes except white light excitation one (WL), while 3 denotes 340, 365 and 385 nm excitation cubes.

mance was recorded for HSI datacubes taken at 400–430 nm excitation, achieving ∼92% average BA ($p < 0.05$ when compared to all lower-wavelength excitations, Fig. 5a heatmap). Among multi-excitation configurations the concatenation-then-normalization approaches (*CN*) yielded higher scores among all tested configurations, reaching ∼97% average BA ($p < 0.05$ when comparing *CN_8* to all non-*CN* approaches). White light illumination had the poorest score, with ∼39%

average BA—lower than the lowest performing 325 nm excitation autofluorescence cube ($\sim$42% BA, p = 0.014).

The improved performance of multi-excitation approach was also challenged with concatenating lower-performing datacubes (340, 365, 385 nm cubes). The concatenated-then-normalized version of preprocessing (*CN_3*) again confirmed the superiority of multi-excitation configurations over single-excitation ones ($p < 0.05$ when compared to the individual cubes comprising the concatenated version).

Visual results of k-NN pixel classification in entire hyperspectral images can be viewed in Fig. 5b for all HSI configurations. A high recall rate for all lichen specimens can be expected from visual inspection in the aforementioned high-performing variants. In the lower-performing configurations—only for certain specimens, if any, the recall rate is expected to be sufficient. The concatenated-then-normalized configuration with 8 cubes tends to exhibit the best outcome. It is important to note that in one of projected application approaches, each specimen can be identified based on the majority of its classified pixels or their average, in which case successful identification of species will be achieved via a recall rate even slightly greater than 50%.

Compared to previous remote sensing and hyperspectral methodologies, our approach offers a more detailed and nuanced analysis of lichen species. While traditional methods focus on broader spectral ranges and reflectance-based identification, the enhanced dimensionality of ME-HSI provides greater granularity in distinguishing species-level differences. This advancement is particularly useful in geographical regions where biodiversity is both rich and complex, and where access to specialized taxonomic expertise or laboratory infrastructure may be limited.

4. CONCLUSION

This study underscores the significant potential of hyperspectral imaging in general, and the multi-excitation version of it in particular, as a promising tool for the identification of various biological specimen including lichen species. In a reflectance mode when samples were illuminated with broadband white light, HSI approach was ineffective. In autofluorescence mode the use of blue light (400-430 nm) was more effective for lichen identification than illuminating the samples with individual wavelengths in the UVA range (300-385 nm). Multi-excitation configurations proved to exhibit superior performance when compared to the single-excitation ones. In the multi-excitation case, the processing approach mattered: concatenating then normalizing the spectra proved to significantly improve the classification performance.

Forthcoming studies will aim to test the applicability of this method in field settings and assessing its robustness in varying environmental conditions. Expanding the study to include a wider range of lichen species and ecological settings would provide additional insights into the versatility of ME-HSI technology. Moreover, integrating machine learning algorithms could enhance data processing, potentially offering real-time identification capabilities. As a result, simple devices suitable for field studies can be produced based on collected spectral response, potentially overcoming current reliance on specialized laboratory techniques. As such it could play a pivotal role in advancing ecological research and promoting sustainable conservation efforts.

5. ACKNOWLEDGEMENTS

We express our gratitude for the financial support received from the European Union grant program (NAR-SAR-IPH-101087403) and the generous funding provided by Sonia & Zaven Akian for the Biolab at the American University of Armenia. Special thanks to Mane Poghosyan for her valuable assistance with initial data acquisition, and to Naira Sargsyan for supplying in-the-field photographs of the lichens.

6. REFERENCES

[1] J. Asta, W. Erhardt, M. Ferretti, F. Fornasier, U. Kirschbaum, P. L. Nimis, O. W. Purvis, S. Pirintsos, C. Scheidegger, C. Van Haluwyn, et al., "Mapping lichen diversity as an indicator of environmental quality," *Monitoring with lichens—monitoring lichens*, pp. 273–279, 2002.

[2] A. Gasparyan and H. J. M. Sipman, "The epiphytic lichenized fungi in Armenia: diversity and conservation," *Phytotaxa*, vol. 281, no. 1, pp. 1–68, 2016.

[3] G. Fayvush, Ed., *Biodiversity of Armenia*, Springer Nature, 2023.

[4] N. Kuusinen, J. Juola, B. Karki, S. Stenroos, and M. Rautiainen, "A spectral analysis of common boreal ground lichen species," *Remote Sensing of Environment*, vol. 247, pp. 111955, 2020.

[5] C. W. Smith, A. Aptroot, B. J. Coppins, A. Fletcher, O. L. Gilbert, P. W. James, and P. A. Wolseley, Eds., *The Lichens of Great Britain and Ireland*, British Lichen Society, London, 2009.

[6] F. Pedregosa, G. Varoquaux, A. Gramfort, V. Michel, B. Thirion, O. Grisel, M. Blondel, P. Prettenhofer, R. Weiss, V. Dubourg, et al., "Scikit-learn: Machine learning in python," *Journal of Machine Learning Research*, vol. 12, pp. 2825–2830, 2011.

[7] S. L. Jacques, "Optical properties of biological tissues: a review," *Physics in Medicine & Biology*, vol. 58, no. 11, pp. R37, 2013.